

HCF PERFORMANCE AND FOD TOLERANCE IMPROVEMENT IN Ti-6Al-4V VANES WITH LPB TREATMENT

Paul S. Prevéy, President, Director of Research (pprevey@lambda-research.com)
N. Jayaraman, Director of Materials Research (njayaraman@lambda-research.com)
Lambda Research, Cincinnati, OH

Ravi A. Ravindranath, Propulsion & Power (ravindranara@navair.navy.mil)
NAVAIR, Patuxent River, MD

ABSTRACT

Mechanical surface treatments that introduce a layer of residual surface compression improve high cycle fatigue (HCF) performance. If the depth of compression extends through the thickness of blade or vane edges, foreign object damage (FOD) tolerance can be dramatically improved. The effect of low plasticity burnishing (LPB) on the HCF performance and FOD tolerance of a first stage Ti-6Al-4V turbine engine vane have been investigated in both tension-tension ($R=0.1$) and fully reversed bending ($R=-1$). Actual vanes from fielded engines and blade-edge feature samples were fatigue tested with FOD simulated by EDM notches.

The fatigue strength for LPB processed blades increased over 4-fold for both vanes and vane-edge feature specimens with FOD 0.020 in. deep, and was undiminished by 0.030 in. deep FOD. Assuming a $K_t = 3$ HCF performance criteria, LPB provided tolerance of FOD up to 0.10 in. deep. The beneficial through-thickness compression was retained even for compressive loading in fully reversed bending. The fatigue and FOD tolerance improvement are shown by linear elastic fracture mechanics modeling to be due to the deep stable compressive layer produced by LPB.

INTRODUCTION

The deep stable layer of compressive residual stress produced by LPB^{1,2,3} has been demonstrated to produce remarkable improvement in damage tolerance, corrosion fatigue, and fretting in a variety of materials. Damage tolerance in IN718,⁴ Ti-6Al-4V,^{5,6} 17-4PH,⁷ and Custom 450⁸ have been studied extensively in laboratory coupons. Mitigation of corrosion pitting damage in aluminum⁹ and steel; and active corrosion in aluminum¹⁰ and austenitic stainless steels⁷ have been reported.

Application of LPB to produce through-thickness compression in the leading edge of a rotating engine component, a Ti-6Al-4V first stage fan blade, produced an order of magnitude improvement in damage tolerance.¹¹ This paper describes the application of LPB to a static engine component, the FOD limited trailing edge of a Ti-6Al-4V first stage low pressure compressor vane.

This investigation was designed to determine the benefit of applying LPB to a first stage Ti-6Al-4V vane to mitigate high sensitivity to damage tolerance on the trailing edge. FOD as small as 0.002 in. has initiated fatigue cracking in the region of the trailing edge fillet shown in Figure 1. The rotating fan blade addressed previously⁶ is subjected to centrifugal tensile loading at a high stress ratio, R ($R=S_{min}/S_{max}$). The static vane, however, is subjected to both bending and torsion with a compressive mean stress producing a large negative R -ratio on the order of -1.9 at the trailing edge. Introduction of a zone of high compression by LPB could then lead to compressive yielding, and a loss of benefit in the statically loaded vane. Finite element modeling of the combined loading indicated a local region of high tension occurring at the site of observed fatigue cracking. The goal of this study was to determine the benefit of applying LPB locally to counter the applied tensile stresses, thus increasing the damage tolerance, and to eliminate fatigue cracking from the trailing edge location. To assess the effectiveness of LPB, actual vanes removed from service were processed and fatigue tested with simulated FOD. Vane-edge feature specimens were used to determine the limits of FOD tolerance improvement and to allow testing in fully reversed bending to assess the effects of compressive loading on the high residual compression from LPB. Fatigue performance was compared to a linear-elastic fracture mechanics based model.

Proceedings 42nd AIAA Aerospace Sciences Meeting
Reno, NV, January 5-8, 2004, Vol. 9, No. 1-4, 2004 Meeting Papers
(LT Paper 252)

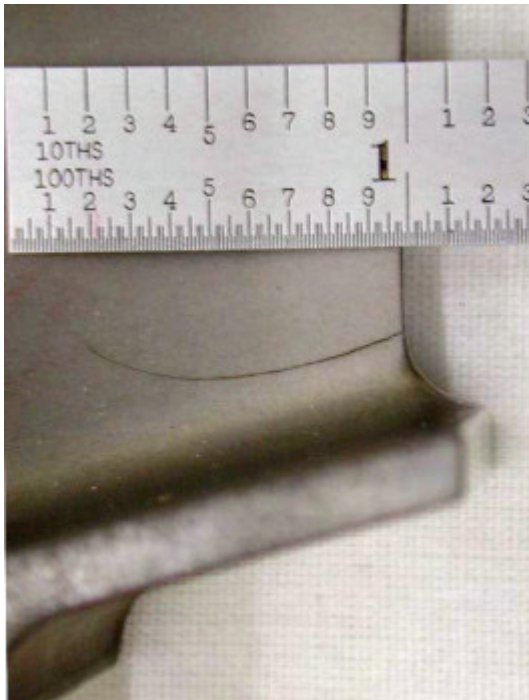


Figure 1 – Fatigue crack initiating from the trailing edge of the Ti-6-4 vane at the point of maximum stress at the trailing edge fillet.

Experimental Methods

Fatigue Samples:

The single vane-edge feature specimen used for initial development of LPB parameters and fatigue testing at R=0.1 is shown in Figure 2. Samples were manufactured from Ti-6Al-4V material (AMS 4911H) purchased as forged plate 25.4 mm (1 in.) thick. The test specimens were all taken with the loading axis parallel to the rolling direction. The material was tested in the annealed condition with a yield strength of 133 ksi, an ultimate tensile stress of 140 ksi, and hardness of 32 HRC. The chemistry of the material obtained is compared in Table I with the nominal chemistry for Ti-6Al-4V.

The sample taper and radius on the edge were designed to match those of the actual vane trailing edge. Tests were performed at 30 Hz, room temperature, in four-point bending under constant stress placing the edge of the blade in tension at R=0.1. Double-edge samples, prepared with symmetrical edges matching the taper and radius of vanes, were tested in fully reversed bending at R=-1. The baseline surface condition was low stress grinding followed by a light buffing to remove grinding marks. All samples were stress relieved at

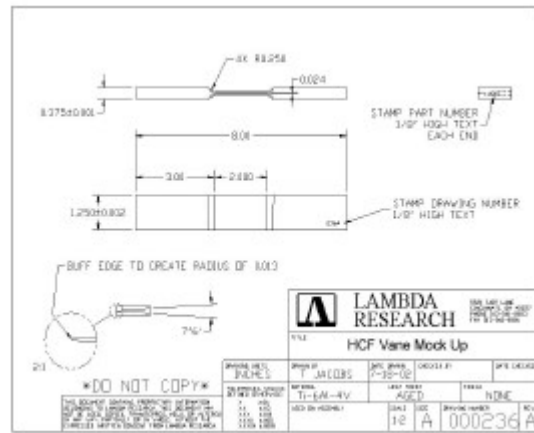


Figure 2 – Single edge vane-edge feature specimen.

Table I
CHEMISTRY Ti-6Al-4V

Test	As-Received	AMS 4911H
Aluminum	6.05%	5.5-6.75%
Carbon	0.015%	0.08%
Iron	0.16%	0.3%
Vanadium	4.00%	3.5-4.5%
Titanium	Remainder	Remainder

700° C for 1 hour to eliminate residual stresses introduced during manufacture.

The vanes available for testing were removed from service. Prior loading histories were not available. A clamping fixture was designed to allow the vanes to be tested in cantilever loading so that maximum tension occurred at the location of observed fatigue cracking on the trailing edge. The location of maximum stress and the local stress distribution produced in cantilever loading were predicted using finite element modeling of the vane, and were found to be comparable to engine service loading. The HCF apparatus is shown in Figure 3. Because of geometric limitations imposed in gripping the vanes, the trailing edge could not be loaded in compression, limiting the vane testing to R>0. The vane fatigue testing was calibrated using electrical resistance strain gages applied at the location of maximum stress to relate the applied load to the actual stress on the trailing edge. Finite element modeling was used to estimate the actual stress at the trailing edge from strain gage grids located as closely as practical to the actual trailing edge radius. The vanes were tested at an R ratio of 0.1, 30 Hz, using constant stress sinusoidal loading.

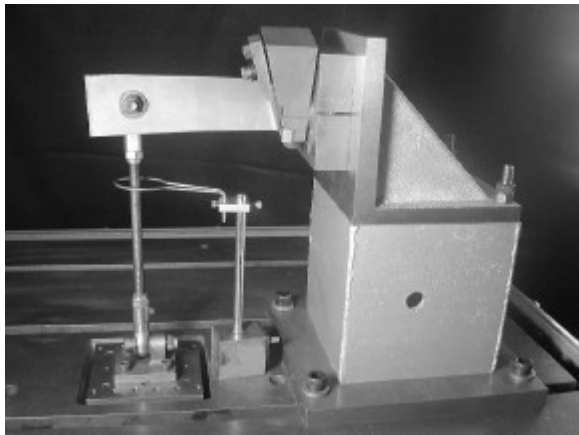


Figure 3 – Cantilever loading HCF test apparatus used for testing vanes at R=0.1.

LPB Processing

Both vanes and vane-edge simulation samples were LPB processed in a conventional four-axis CNC vertical mill. A caliper tool was used to burnish opposing sides of the vane-edge simultaneously, achieving through-thickness plasticity in the nominally 0.030 in. thick leading edge. The LPB parameters including ball size, material, pressure, feed, etc. were determined empirically through a series of trial runs with x-ray diffraction residual stress measurement of the residual stress and cold work distributions achieved. The processing parameters were selected to produce substantial compression on the order of at least -50 ksi through the thickness of the vane leading edge, with high compression on the surface. The processing was then fixed in the code used for CNC machine tool positioning and pressure regulation in the LPB control system. All vanes and samples were then processed essentially identically within the reproducibility of CNC machining practices. The pressures actually achieved for each position of the tool were recorded to files by the LPB control system to allow monitoring of performance and assessment of the uniformity of processing on each vane and sample.

Simulated FOD

FOD was simulated by an EDM notch made with a 0.005 in. thick graphite electrode with depths ranging from 0.020 to 0.100 in. For the vanes, FOD was located at the point of maximum applied stress in cantilever loading. Simulated FOD was cut as an edge notch at the center of the vane-edge specimen gage sections

An EDM notch was selected as a “worst case” method of simulating FOD. Previous detailed studies of actual service generated FOD on Ti-6Al-4V first stage fan blades¹² and 17-4 PH first stage compressor blades⁷ had shown that service FOD comes in every conceivable form, ranging from sharp notches to near spherical indentations. FOD depth distributions are weighted heavily toward small FOD on the order of 0.002 in., with the largest observed depth on the order of 0.02 in. Simulating FOD by impact introduces an arbitrary and difficult to determine residual stress field which can be either tensile or compressive. Previous FOD simulation using indentation⁴ and machined notches¹⁰ in this laboratory indicated residual compression is introduced at the bottom of a machined notch and tension at the shoulders of the indentation. Machined “V”-notches were found to have residual compression at the notch root that tended to prolong fatigue life. EDM produces yield strength tension in the re-cast layer that is typically cracked at the bottom of the notch. EDM also has the advantage of accurate control and repeatability to minimize scatter of the fatigue data.

Residual Stress Distributions

The residual stress and cold work distributions were measured using established x-ray diffraction methods that have been extensively described previously.^{13,14,15} The residual stress distributions achieved by LPB in the trailing edge of both the actual vane and in the vane-edge samples are shown in Figure 4. The span-wise (longitudinal) residual stress distribution is shown as a function of distance chord-wise moving from the trailing edge back along the chord of the vane. For both the vane and vane-edge simulation sample, the stresses are shown at the surface and at depths 0.005 in. and 0.015 in., the nominal mid-thickness of the trailing edge. Compression on the order of -110 to -100 ksi was achieved at a depth of 0.005 in. on the vane simulation samples for a distance of nominally 0.2 in. chord-wise from the trailing edge. Interior compression was lower, on the order of -80 to -50 ksi, at mid-thickness of the vane-edge specimens. Compression on the vanes was lower at the surface, on the order of -50 ksi, from the trailing edge to 0.2 in., which is attributed to the presence of cold work on the order of 35% due to previous glass bead peening of the vanes. The vanes were not stress relieved before LPB processing. Compression at 0.005 in. and at the 0.015 in. mid-thickness depths are quite comparable to that achieved in the vane-edge sample using the same LPB processing parameters and CNC tool control

code.

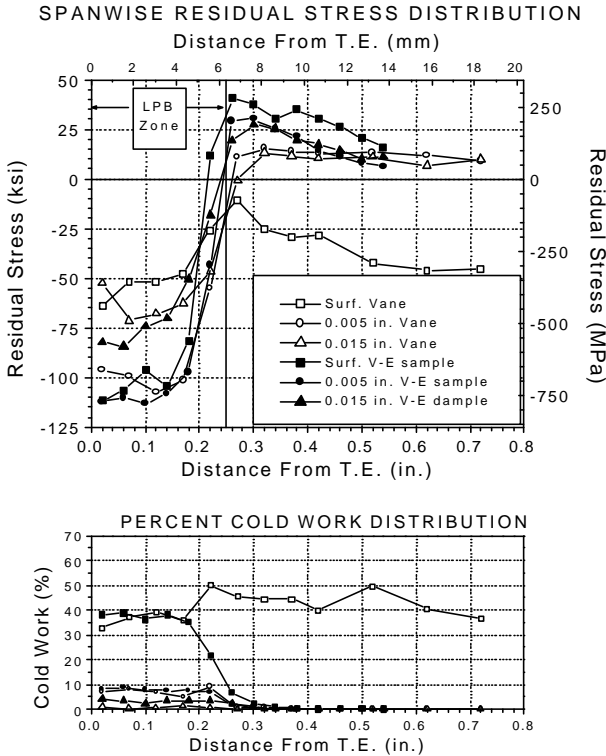


Figure 4 – Span-wise residual stress and cold work distributions at various depths showing through-thickness compression of nominally -75 ksi or more in the vane and vane-edge (V-E) sample trailing edges.

The compensating (equilibrating) tension behind the compressive leading edge is higher in the vane-edge samples than in the actual vanes, reaching 20 to 30 ksi at chord-wise distances beyond the LPB processed 0.25 in., before falling off to nominally 10 ksi at a distance of 0.55 in. In contrast, the actual vane reaches only nominally 12 ksi behind the highly compressive trailing edge. The tension in the vane then extends to greater depths providing equilibration for the compressive edge. This difference in the equilibrating tensile stress distribution behind the compressive edge produced by LPB is attributed to the differences in the geometry of the actual vane and the vane-edge specimen. The greater chord-wise width of the vane provides more material to support the tensile stresses, and lower tensile magnitude is required for equilibrium.

HCF Testing of Vanes

A limited number (32) of Ti-6-4 out of service vanes were available for developing the LPB processing

parameters and fatigue testing. The vanes had been removed from an engine damaged by an unrelated failure causing a number of the vanes to be slightly deformed and damaged near the outboard end. It was therefore recognized at the outset that fatigue testing of this set of atypical vanes, the only actual components available, might not be representative of production vanes. The HCF results shown in Figure 5 show considerable scatter that is attributed to the variability of the blade geometries and to the limited region placed under uniform stress in cantilever loading. The HCF results for the vanes processed with LPB, with or without 0.020 in. FOD, tended to overlap within the scatter band. However, a significant benefit in endurance limit, on the order of nominally 40 ksi, nearly double the endurance limit of the untreated vanes, is evident for the LPB processed vanes. All of the LPB processed vanes failed from the end of the LPB processed zone rather than the FOD introduced at the location of maximum stress. The unprocessed vanes failed from the EDM simulated FOD at lower applied stress, as seen in Figure 5.

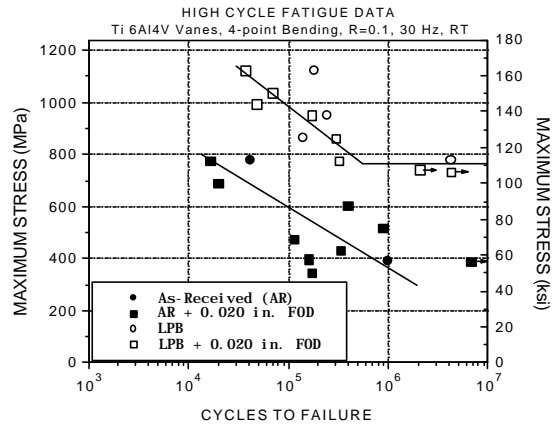


Figure 5 – The effect of trailing edge LPB processing on the HCF performance of Ti-6-4 vanes tested at R=0.1 with and without 0.020 in. deep FOD. The scatter is attributed to the variability of the out-of-service vanes used in the experiment (see text).

The compliance of the vanes, the maximum and minimum vertical deflection under cyclic loading during the constant stress cycle testing, was continuously monitored using an LVDT to observe the growth of fatigue cracks and the effect of LPB induced compression on crack growth. Compliance data are shown in Figure 6 for four specimens representing the four conditions (with and without FOD or LPB) tested at a maximum applied stress of 90 ksi with 0.020 in. FOD. LPB afforded two orders

of magnitude longer life without FOD and a 20-times life increase with FOD. The effect of LPB on crack growth appears to be evident in the final phases of testing in the change in compliance prior to failure. The single attachment for vertical loading shown in Figure 3 through a spherical tie rod end bearing causes the vane to both twist and bend in a complex fashion. The negative change in the Z-axis (vertical) deflection seen for all of the LPB processed vanes is attributed to the combined bending plus torsion loading imposed on the complex vane geometry. It is apparent that LPB significantly affects the growth of the fatigue crack with FOD for the majority of life from nominally 10^5 to 3×10^5 cycles. Similarly, for the LPB vane without FOD, the crack growth appears to be affected from nominally 10^6 cycles to failure at 4.3×10^6 cycles. The compliance data reveal that compression from LPB significantly affects the crack growth rate through the compressive zone, as would be anticipated by simple linear fracture mechanics modeling, and that the extended fatigue life is at least partially attributed to the retardation of crack growth by the compressive layer. Because cracks are present initially in the re-cast layer at the bottom of the EDM notch, initiation is considered to have occurred at the first cycle.

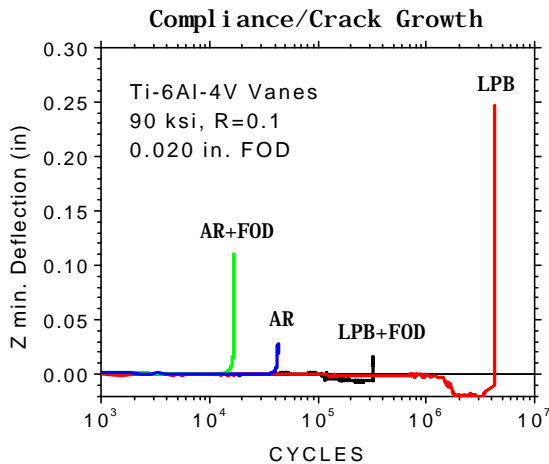


Figure 6 – Compliance data for Ti-6Al-4V vanes tested at 90 ksi as-received (AR) and with and without 0.020 in. deep FOD and LPB processing.

Linear elastic fracture mechanics modeling was undertaken using the AFGROW code assuming a

simple edge notched plate of uniform 0.030 in. thickness. Even with the limitations imposed by the simple geometric models for which closed form stress intensity factor solutions are available, the effect of LPB on fatigue performance is reasonably predicted and shown to be due to the effect of the mean compressive stress induced into the vane edge ahead of the crack. Figure 7 shows the predicted S-N curves for the simple edge notch plate assuming a uniform compressive stress of -100 ksi throughout the thickness. Results are shown for both 0.002 in. deep FOD, the current FOD limit for the vane, and the 0.020 in. deep FOD used for vane testing. Assuming that the smaller FOD might be considered characteristic of surface damage found on vanes removed from service, the predicted fatigue lives for LPB processed vanes, regardless of FOD size, and out-of-service vanes with the smaller FOD are in reasonable agreement with the fatigue data shown in Figure 5. AFGROW predicts a much lower life for the vanes with larger FOD than was actually observed in testing. This may be attributable to deformation that occurred within this high stressed area as a result of the engine failure that lead to the vane removal. The engine failure may have left the region in a state of compressive stress that enhances fatigue performance beyond that predicted for a stress-free model. Further, simple axial loading was assumed in the model. The complex bending and twisting actually imposed on the vane trailing edge by the single point cantilever loading could not be modeled with AFGROW.

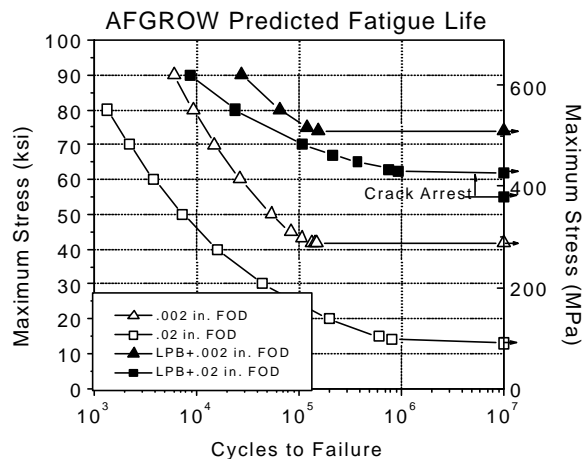


Figure 7 – AFGROW linear-elastic fracture mechanics predictions of high cycle fatigue performance assuming -100 ksi compression in a 0.030 in. thick plate with an edge notch equal to the FOD depths indicated.

Fatigue Testing of Vane-Edge Feature Samples

Testing of fielded vanes provided an important demonstration of the effect of LPB on the fatigue performance of actual components. However, the complications of the complex loading, unknown field history, and the limited number of vanes justified the use of a vane-edge feature sample to generate additional data. Vane-edge feature samples manufactured from the equivalent material with the same radius and taper as the actual vane trailing edge were LPB processed identically producing the residual stress distributions shown in Figure 4 as functions of distance from the trailing edge. Testing in four-point bending provided a large uniformly stressed vane-edge under simple constant stress loading. The four-point bend fixture used to test both the single and double vane-edge samples is shown in Figure 8. Tests were conducted with various FOD depths ranging from 0.020 in. to a maximum of 0.060 in.

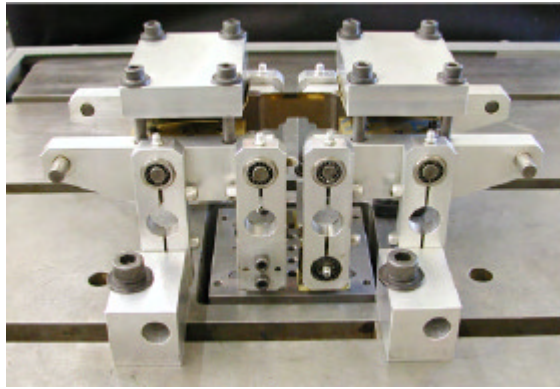


Figure 8 – Four-point bend fixture used for Ti-6-4 vane-edge feature samples, both single-edge (R = 0.1) and double-edge (R = -1), shown with a single-edge sample positioned for testing.

Because the static vane is loaded at an R ratio of -1.9 during engine service, the possibility existed

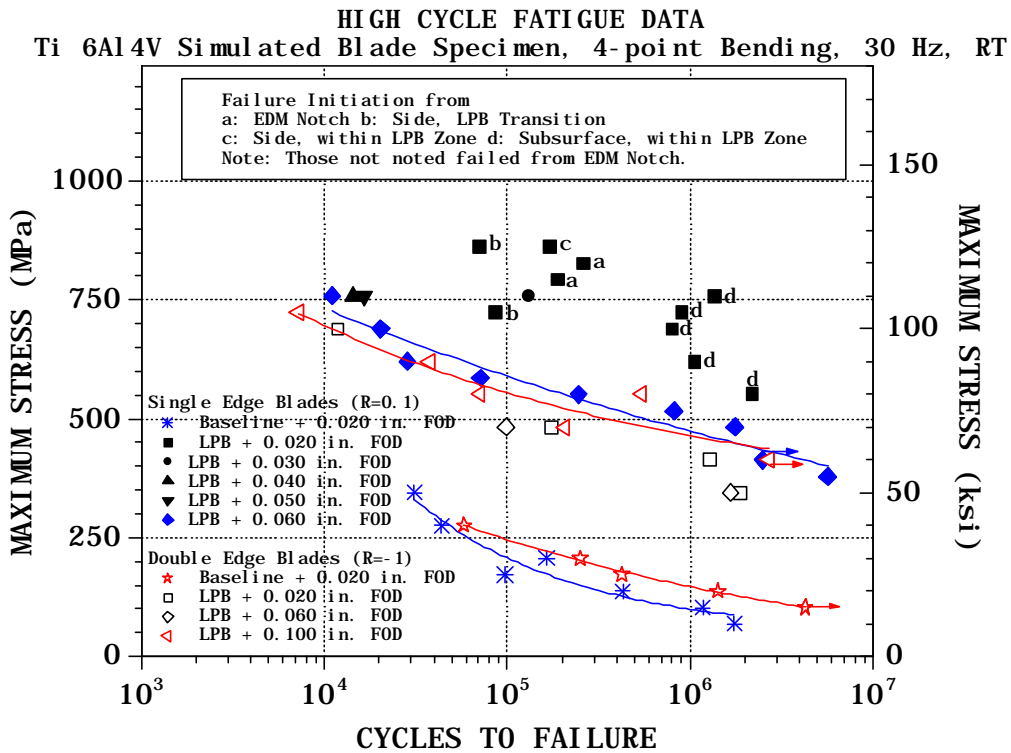


Figure 9 – S-N curves for single-edge and double-edge vane-edge feature samples tested with and without LPB and FOD depths from 0.020 to 0.100 in.

that the already highly compressive trailing edge would yield in compression during the compressive portion of the loading cycle, reducing or eliminating the compressive residual stresses and the resulting benefit in fatigue performance. Testing at R=-1.9 was not feasible in bending, and axial testing was not possible for the sample dimensions required for equilibrium below the deep LPB compressive layer. Therefore, a double edge four-point bend specimen with symmetrical opposing trailing edge geometries identical to that shown in Figure 2 was fabricated. The double edge specimen was tested in fully reversed bending (R=-1) so that the compressive LPB processed zone was driven to the same magnitude of compression as tension on each cycle.

The results of both the single-edge and double-edge tests are summarized in Figure 9. FOD of 0.020 in. drastically reduced the fatigue life of both single-edge (R=0.1) and double-edged (R=-1) specimens to nominally 10 ksi, with slightly higher performance for the fully reversed bending. It proved extremely difficult to achieve failure from the smaller FOD dimensions in the LPB processed double-edge sample, as fatigue cracking typically initiated from the boundaries of the LPB zone.

For both the single- and double-edge sample it was difficult to obtain failures out of the FOD until the FOD size was substantial. FOD as large as 0.060 in. did produce uniform failure from the FOD with evident plasticity occurring at the crack tip in the LPB processed samples. Fatigue strength of nominally 50 ksi at 10⁷ cycles was achieved with 0.060 in. deep FOD for the single edged specimen tested at R = 0.1. An endurance limit on the order of 40 ksi was achieved for the same depth of FOD for the double edge sample at R=-1. The HCF endurance limit achieved as a function of FOD size for the single-edge sample at R=0.1 are summarized in Figure 10. A nearly linear relationship was observed with endurance limits ranging from nominally 80 to 50 ksi for FOD depths from 0.020 to 0.060 in.

Fatigue results for the vane-edge feature samples indicate no significant reduction in fatigue performance as a result of testing in fully reverse bending (R=-1) as compared to tension-only testing (R=0.1) The data further indicate that damage tolerance for the vane could be increased to as much as 0.060 in. or even 0.100 in. from the current 0.002 in. limit, and still achieve fatigue performance in excess of the Kt=3 criteria typically employed in HCF limited design.

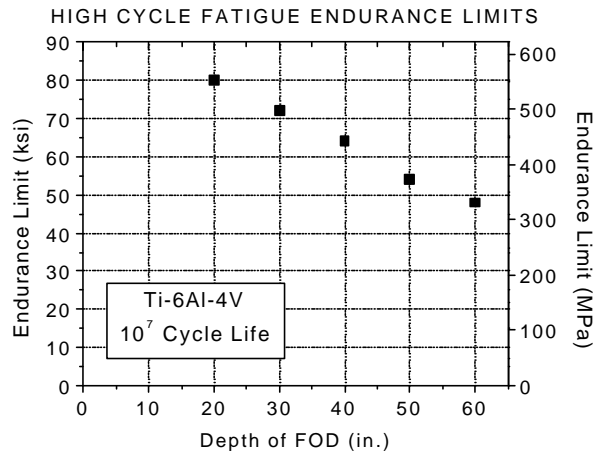


Figure 10 – HCF endurance limit for LPB processed Ti-6-4 vane-edge feature samples as a function of FOD depth.

The effect of fully reversed loading on the magnitude of compression retained in the LPB treated edge of the double-edge samples was assessed by performing residual stress measurements after fatigue loading to failure. Measurements were made in the same manner as for Figure 4 after both high and low stress testing at a location in the uniformly stressed gage section away from the deformation zone near the fatigue crack. The results are shown in Figure 11 for samples tested to failure at 11, 875 cycles at 100 ksi and 1,881,563 cycles at 50 ksi. Comparison to the residual stress distributions shown in Figure 4 before cycling indicates only a loss of perhaps 10 ksi at the lower stress level and 35 ksi at a maximum applied stress level, chosen to be high enough to cause failure in the low cycle fatigue regime. The post-test residual stress data show that the compression from LPB is reduced by compressive loading, but was retained sufficiently to provide substantially improved fatigue performance.

The effect of R-ratio on fatigue performance was investigated using the AFGROW linear elastic fracture mechanics modeling code with the same assumptions described previously. The S-N curves for R=0.1 used for actual vanes and single-edge specimens, R=-1 (fully reversed) used with the double-edge specimens, and R=-1.92, the reported R-ratio experienced at the trailing edge in service, were calculated. The results shown in Figure 12 indicate that the high mean compression introduced by LPB greatly reduces the effect of the external mean stress and therefore the applied stress R-ratio on fatigue life. With the high compression from LPB, shown in solid symbols, the S-N curves are

virtually identical for $R=0.1$ or $R=-1$, and show infinite life for maximum stress levels below nominally 52 ksi regardless of the applied stress R -ratio. AFGROW predicts initial fatigue crack growth as indicated above nominally 50 ksi for the two different R -ratios, but crack arrest resulting in infinite life. In the absence of the high internal compressive stress, a difference in fatigue life is evident with R -ratio, but the difference is hardly significant from an engineering design standpoint. Either R -ratio without LPB results in an endurance limit just above 10 ksi. The model predicts infinite life for an LPB processed vane with 0.020 in. deep FOD in engine service at the actual maximum stress and -1.92 R -ratio reported, and a life of only 10^4 cycles in the absence of LPB.

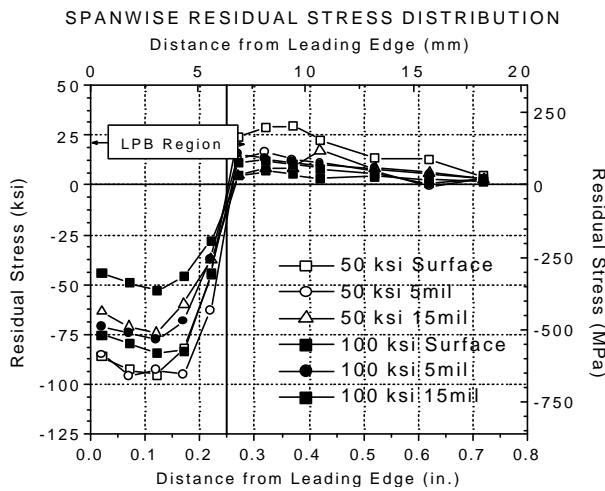


Figure 11 – Post fatigue test residual stress distributions for double-edge vane edge feature samples tested at $R = -1$ at maximum stresses of 100 and 50 ksi, showing substantial retention of the LPB compressive zone.

CONCLUSIONS

LPB processing of a Ti-6Al-4V first stage vane, a static fatigue critical engine component, has been demonstrated to improve damage tolerance by an order of magnitude and to withstand cyclic loading in compression in fully reversed bending. Specially:

- LPB processing of fielded Ti-6Al-4V vanes with a current trailing edge damage tolerance 0.002 in. resulted in a ten-fold increase in damage tolerance to at least 0.020 in.
- The fatigue strength of the trailing edge of LPB

processed vanes doubled, from nominally 40 to 80 ksi.

- The beneficial compression and the fatigue benefit of LPB are not lost when the vane is cycled into compression at stress levels producing HCF failures, even in the high-stress low cycle fatigue regime.
- The minimal effect of R -ratio on fatigue life with high residual compression from LPB was confirmed with linear elastic fracture mechanics.
- FOD up to 0.060 in. was tolerated with fatigue strength of 60 and 50 ksi for $R = 0.1$ and $R = -1$, respectively. The results were corroborated with linear elastic fracture mechanics modeling for the residual stress level and FOD sizes investigated.
- LPB has been demonstrated to provide significant damage tolerance in non-rotating components cycled into compression, offering a significant reduction in the cost of aircraft ownership and improved fleet readiness.

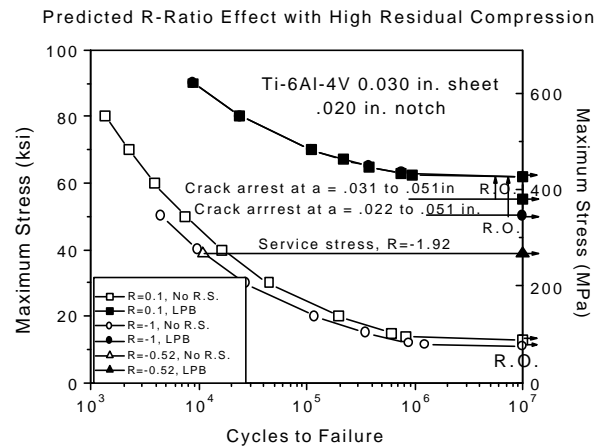


Figure 12 – HCF S-N curves calculated with AFGROW for 0.020 in. deep FOD and R -ratios of 0.1, -1.0 and -1.92 showing no significant effect of applied stress R -ratio with high residual compressive stress of -100 ksi.

ACKNOWLEDGEMENTS

The support of this research with funding through the NAVAIR SBIR program (Contract No. N68335-02-C-0384) is gratefully acknowledged. D.

Hornbach and P. Mason along with the Lambda Research staff contributed the residual stress and fatigue data and many hours of diligent effort that made this work possible.

REFERENCES

- 1 T. Gabb, J. Telesman, et.al., (2002) "Surface Enhancement of Metallic Materials", *Advanced Materials & Processes*, ed. Peg Hunt, ASM, Materials Park, OH, January, pg. 69-72.
- 2 "Longer Life with Low Plasticity Burnishing", *Manufacturing Engineering*, ed. Brian Hogan, SME, December 2001, pg. 34-38.
- 3 U.S. Patents No. 5,826,453 (Oct., 1998) and 6,415,486 (Jul., 2002), other US and foreign patents pending.
- 4 Paul S. Prev y, et.al., (2000) "FOD Resistance and Fatigue Crack Arrest in Low Plasticity Burnished IN718", Proc. 5th National High Cycle Fatigue Conference.
- 5 Paul S. Prev y, et. al., (2001) "The Effect of Low Plasticity Burnishing (LPB) on the HCF Performance and FOD Resistance of Ti-6Al-4V," Proc. 6th National Turbine Engine High Cycle Fatigue (HCF) Conference, Jacksonville, FL, March 5-8.
- 6 Paul S. Prev y, Doug Hornbach, John Cammett, and Ravi Ravindranath, (2002) "Damage Tolerance Improvement of Ti-6-4 Fan Blades with Low Plasticity Burnishing," Proc. 6th Joint FAA/DoD/NASA Aging Aircraft Conference, San Francisco, CA, Sept 16-19.
- 7 NAVAIR SBIR Contract N68335-02-C-0384 "Affordable Compressor Blade Fatigue Life Extension Technology", monthly report dated March 11, 2003.
- 8 Lambda Research unpublished IR&D Report, Jan. 2003.
- 9 Paul S. Prev y and John T. Cammett, (2002) "The Influence of Surface Enhancement by Low Plasticity Burnishing on the Corrosion Fatigue Performance of AA7075-T6," Proc. 5th International Aircraft Corrosion Workshop, Solomons, Maryland, Aug. 20-23.
- 10 Paul S. Prev y and John T. Cammett, (2002) "Restoring Fatigue Performance of Corrosion Damaged AA7075-T6 and Fretting in 4340 Steel with Low Plasticity Burnishing," Proc. 6th Joint FAA/DoD/NASA Aging Aircraft Conference, San Francisco, CA, Sept 16-19.
- 11 Paul S. Prev y, Doug Hornbach, John Cammett, and Ravi Ravindranath, (2002), "Damage Tolerance Improvement of Ti-6-4 Fan Blades with Low Plasticity Burnishing," Proc. 6th Joint FAA/DoD/NASA Aging Aircraft Conference, San Francisco, CA, Sept 16-19.
- 12 P. Prev y, D. Hornbach, R. Ravindranath, J. Cammett, (2003), "Application of Low Plasticity Burnishing to Improve Damage Tolerance of a Ti-6Al-4V First Stage Fan Blade," Proc. 44th AIAA/ASME/ASCE/AHS Structures, Structural Dynamics, & Materials Conf., Norfolk, VA, April 7-10.
- 13 P.S. Prev y, ASM Metals Handbook, Vol. 10, ASM, Metals Park, OH, 380-392
- 14 M.E.Hilley, ed. (2003) Residual Stress Measurement by X-ray Diffraction, S 784, SAE, Warrendale, PA.
- 15 Noyan and Cohen, J.B. (1987) Residual Stress by Diffraction and Interpretation, Springer-Verlag, NY.